Microplastics and Nanoplastics

RESEARCH

Open Access

Environmental degradation and fragmentation of microplastics: dependence on polymer type, humidity, UV dose and temperature

Patrizia Pfohl[1†], Katherine Santizo[1†], Joana Sipe[2,3], Mark Wiesner[2], Sam Harrison[4], Claus Svendsen[5] and Wendel Wohlleben[1*]

Abstract

Depending on the environmental compartment, plastics are subjected to various stressors, including UV light, water, microbial exudates (enzymes), and temperature. Among these, stress on plastics from photo-chemical processes was identified as a leading exposure pathway of plastics, e.g., in the atmosphere or on the water surface. While the focus of earlier studies mainly was on deterioration of the chemical and mechanical properties, more recent studies demonstrate how photo-oxidation leads to fragmentation and release of secondary micro- and nanoplastic fragments, as well as low-molecular weight species. These studies tend to focus on a single exposure condition and a limited number of polymer types. Therefore, this study focuses on systematically evaluating the influence of temperature and relative humidity during simulated UV exposure on the fragmentation and degradation of five types of pristine microplastic powders: polypropylene, low density polyethylene, polyamide 6, high impact polystyrene and thermoplastic polyurethane. We quantified the dose-dependent release of water-soluble organics, as well as secondary micro- and nanoplastics (including their particle size distributions) and found that the polymer identity dictated the type and quantity of species released rather than the aging protocol. With this systematic assessment the generated data can be used in mechanistic microplastic fragmentation models to determine fragmentation rates and fragment size distributions.

Keywords Microplastics, Fragmentation, Degradation, Photolysis, Environmental stresses

[†]Patrizia Pfohl and Katherine Santizo contributed equally to this work.

*Correspondence:
Wendel Wohlleben
wendel.wohlleben@basf.com
[1]BASF SE, Carl-Bosch-Str. 38, 67056 Ludwigshafen, Germany
[2]Department of Civil and Environmental Engineering, Duke University, Durham, NC 27708, USA
[3]Ira A Fulton Schools of Engineering, Arizona State University, Tempe, AZ 85296, USA
[4]UK Centre for Ecology and Hydrology, Lancaster Environment Centre, Lancaster, UK
[5]UK Centre for Ecology and Hydrology, Wallingford, Oxfordshire, UK

Introduction

The presence of microplastics in the environment has been clearly proven by the large number of field studies conducted in recent years [1–4]. Still, the fate and behavior of microplastics, once released into the environment, remains unclear [5–7]. Researchers are currently trying to fill knowledge gaps regarding their persistency [8, 9] and further degradation and fragmentation to potentially harmful nanoplastics or other species [10–13]. However, long-term field experiments come with several challenges, e.g. appropriate sampling [14, 15],, cross-contamination [16, 17], understanding the complexity of environmental impacts [18, 19], and micro- and nanoplastic extraction from complex environmental media [20, 21]. The assumption that microplastics can persist for several decades requires additional accelerated lab-experiments to simulate and understand environmental fragmentation and degradation mechanisms of microplastics, thereby providing data for the parameterization of environmental fate and exposure models [22, 23].

Environmental degradation of microplastics is based on several complex mechanisms that depend on the combination of stresses dominant in a particular environmental compartment. The polymer composition of microplastic particles is of high importance for several environmental processes like hydrolysis [24, 25], photolysis [26, 27], and enzyme-mediated reactions [28, 29], which can induce chemical degradation such as oxidation, crosslinking and chain cleavage [30, 31]. This chemical degradation directly impacts the susceptibility to fragmentation under mechanical stress [32–34]. Literature indicates the importance of environmental stressors for secondary micro- and nanoplastic release and also highlights dissolved organic carbon (DOC) as an additional release pathway (Fig. 1) [7, 35–39]. Stress on plastics from ultraviolet (UV) exposure is commonly evaluated due to its potential to degrade plastics at faster rates than other environmental stresses [40]. Earlier studies looked at the mechanism of chain scissions in polymers due to photo-oxidation and photolysis, providing insight into molecular changes that promote the deterioration of useful properties of macroscopic plastic parts [41, 42]. In turn, more recent studies demonstrate how photo-oxidation leads to fragmentation and degradation of microplastics [43–45]. These studies tend to focus on one exposure condition (a single stress) and a limited number of polymers, but in reality combinations of the aforementioned stressors contribute to degradation and fragmentation of microplastics in the environment. Overall, there is a lack of harmonized methods to obtain microplastic fragmentation and degradation rates under various environmental conditions, since up to now few studies addressed this issue [8, 32, 46, 47]. Environmentally realistic fragmentation modelling requires release rates of fragmented particles for single and combined stresses, as well as extensive characterization and size distribution analysis for a large range of polymers.

Therefore, this study focuses on systematically evaluating the influence of temperature and relative humidity during UV exposure on five pristine microplastic powders and characterizing the powders and their release products at specific time intervals. We recently reported

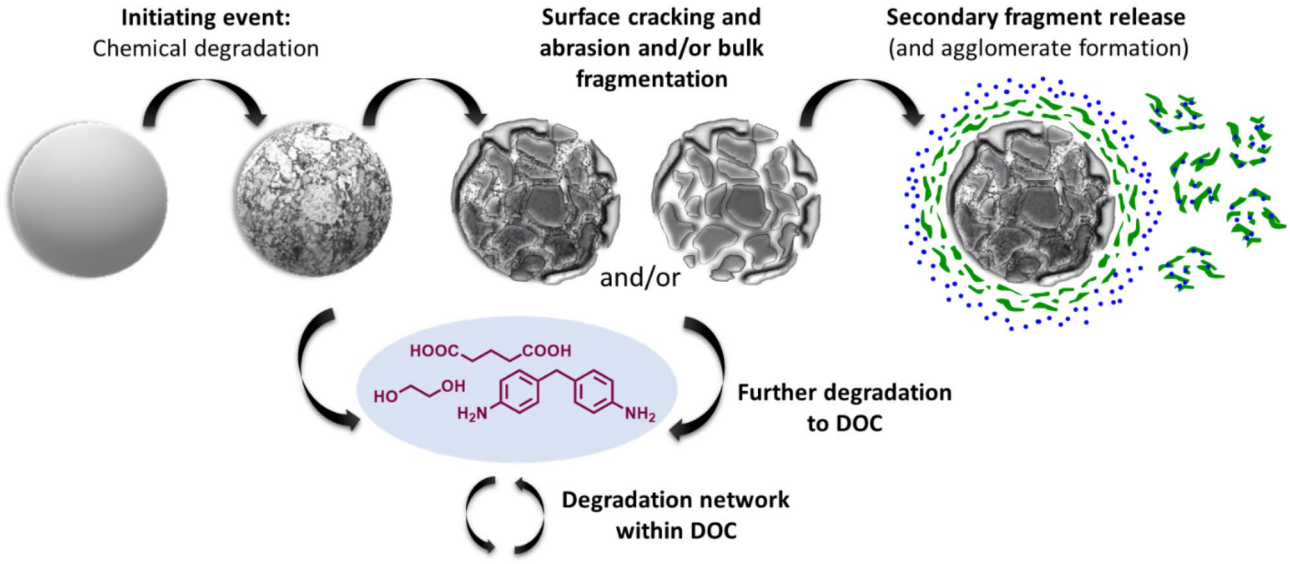

Fig. 1 Schematic representation of fragmentation and degradation steps during the aging of microplastics in the environment. Due to chemical degradation, microplastic particles are more prone to mechanical stress, leading to surface abrasion or bulk fragmentation and secondary micro- and nanoplastic release, which might tend to form agglomerates. In parallel, dissolved organic carbon constitutes an additional release pathway forming its own degradation network [35–38].

how to measure fragmentation rates to secondary micro- and nanoplastic fragments and their dissociation into dissolved organics [36], by specifically adapting the NanoRelease protocol [48, 49] to determine release rates from polyamides (PA) and thermoplastic polyurethanes (TPU), but we only applied one dry UV aging protocol. Here, we additionally varied humidity and temperature conditions, and investigated microplastics from a single grade of each of the following materials: low-density polyethylene (LDPE), polypropylene (PP), and high impact polystyrene (HIPS) artificially aged with three different protocols. The goal was to cover a broad range of different types of polymers. Polyolefins are the most largely used plastic types (approx. 50% of the European plastics consumption) [50]. HIPS and TPU have a more complex chemical composition (including phase separation) and therefore a higher potential for fragmentation [51]. One TPU and one PA that were already investigated in our previous study were included as benchmark materials [36]. We determined the chemical degradation, as well as release rates for secondary micro- and nanoplastic fragments, and for low-molecular-weight water-soluble organics. The generated data can be used for the parameterization of environmental fate models, such as the new open-source plastic fragmentation model FRAGMENT-MNP [52].

Materials

An injection-molding grade polyamide-6 (PA-6) acquired from BASF SE with intended use in carpets or in compounding, an aromatic thermoplastic polyurethane containing ether bonds in the polyol phase (TPU: TPU_ether_arom in our previous study [36]) with intended use in cable sheathing, hoses, and films acquired from BASF Polyurethanes, polypropylene (PP; reactor elastomer modified) for application as an automotive coating acquired from Borealis, low density polyethylene (LDPE) acquired from LyondellBasell (relatively low molar mass) with intended use in toys, caps and closures, engineering parts, and sports and leisure equipment, and high impact polystyrene (HIPS) acquired from Formosa Chemicals & Fibre Corporation with intended use in 3D filament printing were used. PA-6, TPU and LDPE are specified as containing no additives. With the UV stabilizing additives contained, this PP grade is quite stress resistant and therefore serves as a negative control for UV stress. As described in our previous publication [36], the PA-6 powder (< 80 µm) was produced for Selective Laser Sintering by BASF SE. Cryo-milling and sieving of granules from TPU (< 315 µm) [36], PP (< 500 µm), and LDPE (< 500 µm) as well as HIPS filament (< 500 µm) generated polydisperse polymer powders. Selected particle properties and images are provided in the Supporting Information (SI Fig. 1, SI Table 1 and in our previous study [36]).

Methods

Artificial UV aging following ISO 4892 (relative humidity = 50% or 75%) and Kalahari protocol

Three aging conditions, with varied UV intensity, temperature, and humidity, were applied for the investigations in this study (SI Table 2). Artificial aging was performed using an Atlas SUNTEST XXL conforming to ISO 4892 standardized conditions (Sunlight spectrum, UV intensity of 60 W/m^2 (max. deviation ± 7.0%) in the wavelength range of 300–400 nm, Black Standard Temperature (BST) of 65 °C) [36, 53]. Complementary to our previous study the relative humidity (RH) was varied (50% vs. 75%) and monitored. The third UV aging protocol was applied in an Atlas SUNTEST XLS + and is known as the "Kalahari protocol", which is more aggressive (BST of 90 °C, RH = 28%, measured, similar to conditions in the Kalahari desert) and is the preferred testing method for automotive coatings [54]. The same sample preparation in each of the aging protocols was applied as described before [36]. In short, thin powder layers (0.7 mm height, duplicates of each polymer) were artificially aged in a petri dish for 1000, 1500 and 2000 h (216, 324, 432 MJ/m^2 for ISO4892 and for Kalahari) and partially covered with quartz glasses. The aged microplastics were analyzed regarding their surface chemistry via attenuated total reflectance Fourier-transform infrared spectroscopy (ATR FT-IR), their surface texture via scanning electron microscopy (SEM), and their molar mass distribution via gel permeation chromatography (GPC). Additionally, their thermal properties were analyzed via differential scanning calorimetry (DSC) and their particle size distributions via Fraunhofer light scattering.

Sampling via ISO22293:2020 NanoRelease protocol

As described before, the NanoRelease protocol can be used for sampling and size-selective quantification of micro- and nanoplastic fragments released from polymers after weathering [36, 48]. Similar to our previous study, 0.45 g of pristine or UV aged polymer powder were dispersed in 2 mL of ultrapure water with surfactant (sodium dodecyl sulfate, SDS, 1 g/L) and treated with 1 h of ultrasonication (Sonorex Digital 10P, Bandelin, 100%, 20 °C). For primary particle removal, the dispersion was then transferred to a centrifuge vial (Polypropylene 11 × 60 mm, Beckman Coulter) and left for 5 min for 1-g-sedimentation. The supernatant containing secondary fragments was analyzed by analytical ultracentrifugation with a refractive index detector (AUC-RI, secondary nanoplastics from 0.01 µm to 1 µm) and a single particle counter (secondary microplastics from 1 µm to 139 µm) [36]. For the release rate assessment of low molecular weight organics, the same procedure was applied without adding surfactant and with an additional 0.02 µm filter

step (Anotop®, Whatman®) to measure the concentration of dissolved organic carbon (DOC).

Details of the experimental conditions for ATR FT-IR, GPC, DSC, SEM, Fraunhofer light scattering, AUC-RI, single particle counter and DOC are described in the Supporting Information (SI).

Results and discussion

The intensity of chemical degradation depends on the UV aging conditions and on the polymer type

Chemical degradation of polymers leads to polymer chain cleavage and consequently to a molar mass reduction or crosslinking and consequently to a molar mass increase depending on which mechanism is predominant [30, 55]. Very specifically for UV aging of polymers, the carbonyl index increases by autoxidation and Norrish reactions [56, 57]. According to literature, amorphous phases in polymers are more affected by UV degradation than crystalline phases, leading to the assumption that environmental aging of microplastics results in an enrichment of highly crystalline regions in microplastics [35, 38, 58]. In this study we considered the carbonyl index, the molar mass, and the crystallinity of microplastics to be the most relevant polymer properties to monitor chemical degradation (Fig. 1, initiating event) induced by different UV aging protocols.

UV aging led to an increase of the carbonyl index for four of the five polymers investigated in this study, in all three aging protocols (Fig. 2a, SI Table 3). The negative control PP was the only exemption, showing no significant differences in the carbonyl index, neither by variations of the UV aging protocol nor by the exposure duration. This is to be expected due to the UV stabilizing additives used in this polymer [59]. The heat map plot (Fig. 2a) highlights the differences in the UV aging protocols and exposure duration for PA-6, HIPS, LDPE and TPU. In general, independent from the polymer type and the UV aging protocol, an increase of the carbonyl index was detected with increasing exposure duration. However, the resulting changes in the carbonyl index strongly depended on the polymer type. Although comparing absolute carbonyl index values across different polymers should be approached with care due to their dependence on the intensity of the reference peak [60], the different trends with increasing time of aging can still be observed and compared. The aromatic polymers HIPS and TPU showed the highest values, followed by PA-6 and LDPE with significantly lower values, but still higher than the negative control PP. HIPS and TPU were also the materials with the most intense yellow discoloration, which can be explained by the generation of quinoid chromophore structures during UV irradiation [61]. The systematic increase of the carbonyl index of LDPE with increasing UV aging time depended on humidity during UV aging. Under 75% RH the carbonyl index was lower compared to the other UV aging protocols (Fig. 2a), indicating that the presence of water molecules slowed down the formation of new carbonyl groups. Low molecular radicals (such as hydroxyl radical formed in the presence of water) can induce termination reactions and hence stop

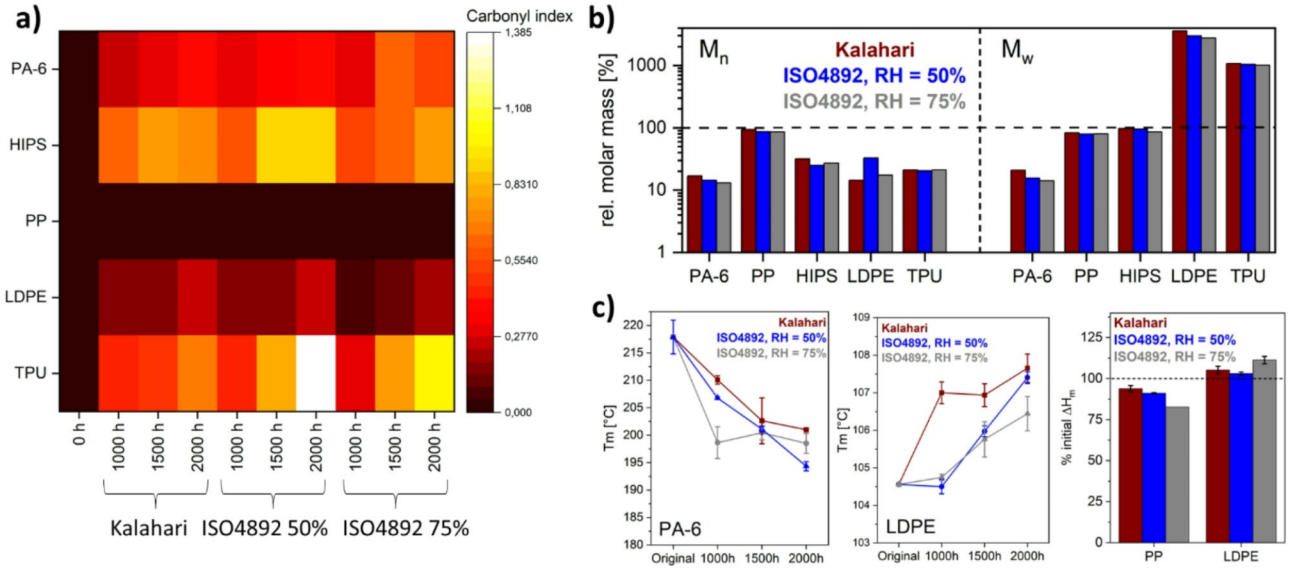

Fig. 2 Changes in chemical properties observed after UV-humidity-temperature aging of different types of microplastics; (**a**) carbonyl index for all polymers, all UV aging protocols and all timepoints; (**b**) molar mass relative to pristine for all polymers after 2000 h UV aging for all aging protocols: left part are number based molar masses M_n, right part are mass based molar masses M_w; (**c**) melt point T_m decrease for PA-6, melting point T_m increase for LDPE with increasing UV irradiation time (2nd heating curve), and changes in melting enthalpy ΔH_m for PP and LDPE after 2000 h UV aging in all aging protocols (1st heating curve)

the propagation) [62]. Temperature changes, tested in this study with the Kalahari protocol, seemed to have no influence on the formation of carbonyl groups on the surface of LDPE microplastics, but the Kalahari protocol was also the one with the lowest relative humidity of 28%. The carbonyl index of PA-6 was constant over almost all aging protocols and exposure duration (Fig. 2a). A slightly higher carbonyl index was only observed after 1500 and 2000 h of UV aging with 75% RH, demonstrating that in the case of PA-6 the presence of water molecules supports the formation of new carbonyl groups. PA-6 is known for its high water uptake [36, 63]. Temporal dependency was also observed for HIPS and TPU (Fig. 2a). However, for the aromatic microplastics the highest values for the carbonyl index were obtained with the ISO 4892 50% RH protocol, indicating that higher temperatures and water content together do not favor the formation of carbonyl groups. In summary, we observed that a higher temperature was not decisive for the increase in the carbonyl index, but the presence of water had a more severe impact on the formation of carbonyl groups, especially when the microplastic type is susceptible.

UV aging also led to a reduction of the microplastic molar masses for all polymers except LDPE and TPU, but the differences between the applied UV aging protocols were less pronounced than for the carbonyl index (Fig. 2b, SI Table 4, SI Table 5). For PA-6, PP, and HIPS, no UV-induced crosslinking was observed, while for LDPE and TPU crosslinking was predominant and led to the formation of gel fractions. The presence of a gel fraction indicates that the polymer is crosslinked beyond the gel point. The weight-average molar mass of a sample crosslinked beyond the gel point is infinite while its number-average molar mass remains finite. With knowledge of the weight fraction of gel, the weight fraction of sol, the molar mass distribution of sol, one can provide a conservative estimate of the molar mass averages of the whole sample by assuming the gel fraction molar mass must exceed the molar mass exclusion limit of the GPC column used (in reality, the weight-average molar mass of the gel is infinite). These estimates for LDPE and TPU are provided in SI Table 5; Fig. 2b. PP showed the lowest molar mass reduction of maximum 20%. For PA-6, the molar masses were reduced by over 80% (number M_n and mass-based M_w). For HIPS, M_n was reduced to a much higher extent (60–80%) than M_w (< 20%) and the polydispersity was increased (SI Table 4), implying preferred formation of shorter chains (chain cleavage closer to their terminal chain ends) instead of statistic chain cleavage at any position in the polymer chain. Considering that HIPS is a rubber (butadiene) modified PS this could also mean that one of the two polymer types contained was more affected than the other. Analogous to the observations for the carbonyl index, the molar mass reduction for PA-6 was more pronounced in the presence of water. For LDPE and TPU the molar masses and the weight-fractions of only the soluble polymer could be measured by GPC (SI Table 4), but as described above, molar mass averages of the whole samples were estimated conservatively (SI Table 5). The underlying crosslinking reaction mechanisms for the investigated TPU were described in our previous publication and are based on the recombination of radicals or peroxide bridges in the polyether-polyol soft segments [36]. Similar crosslinking mechanisms are expected for LDPE, since crosslinks are usually formed by the recombination of radicals within the polymer chain (P-P or P-O-O-P crosslinks) [64].

For the comparison of the thermal properties, the melting points (T_m) of LDPE, PP and PA-6 were compared after treatment with the three UV exposure protocols (Fig. 2c, SI Fig. 2 and SI Table 6). For HIPS, the glass transition temperature (T_g) was in the focus (SI Fig. 2, SI Table 6). The DSC curves of TPU showed no pronounced T_g or T_m and will therefore not be discussed. The 1st heating curve shows the polymer state directly after the thermal pre-treatment (UV aging at specific temperatures), while the 2nd heating curve (commonly used for DSC data evaluation and comparison) shows the polymer properties after deletion of the thermal prehistory and rearrangement of chains and crystallites but still provides information on changes in the polymer properties due to aging.

The UV treatment and especially the presence of water during UV aging had an influence on the T_m of PA-6. With increasing aging duration and humidity, the melting temperature was reduced by up to 23 °C. In addition, the increasing water content also led to a reduced melting enthalpy ΔH_m (SI Fig. 3). We interpret that shorter polymer chains (confirmed by GPC measurements) and the presence of water molecules inside of PA-6 particles lead to higher chain mobility and therefore to a reduction of the T_m and the crystallinity [65, 66]. The T_m of LDPE was slightly increased by around 3 °C (Fig. 2c, 2nd heating curve) and by around 7 °C (1st heating curve) after 2000 h of UV aging. This change might indicate the degradation of the amorphous phases leading to a slight increase in crystallinity, in accord with findings in literature [67, 68]. This interpretation was also confirmed by the analysis of ΔH_m in the 1st heating curve before and after UV treatments (Fig. 2c), showing an enthalpy increase. However, a decrease of ΔH_m is observed in the 2nd heating curve (SI Table 6). Additionally, since UV aging was done at high temperature, chain rearrangement by tempering could also have led to the observed melting point increase [68, 69]. Even though the molar mass reduction for PP was low, the T_m and ΔH_m of PP were reduced with increasing UV aging time, indicating polymer chain cleavage

and consequently improved chain mobility (Fig. 2c, SI Figs. 2 and 3, SI Table 6). The investigation of the T_g in HIPS showed the same trend: higher chain mobility due to polymer chain cleavage results in a T_g reduction with increasing UV aging duration (SI Fig. 2, SI Table 6). In general, it is known, that degradation of the amorphous phases happens before the degradation of the crystalline phases, because of their lower compactness and therefore reduced stability [35]. The polymer degradation leads to DOC release and volume loss. But in the case of a fully amorphous or fully crystalline polymer, this theory would not lead to an enrichment of crystalline phases. The PA-6 investigated here might be an example for a very crystalline polymer, while HIPS is completely amorphous. In both cases no crystallinity increase was observed. Changes of the ratio amorphous: crystalline therefore depend on the polymer type (and their chain properties, such as crystallinity, but also glass transition) and on the environmental conditions (improved chain mobility at higher temperature).

Qualitative SEM images of the investigated microplastics and their surfaces before and after aging were taken to gain insights into possible fragmentation mechanisms (Fig. 1, surface ablation vs. bulk fragmentation) [35, 38]. SI Figs. 4 and 5 display all particles throughout the three aging protocols at 2000 h compared to the pristine particles. In general, the images show that the features in each of the microplastic types were similar across the three aging protocols. Statistical changes in the surface texture were observed for all polymer types (SI Fig. 5). PP exhibited only minimal micro-cracks after 2000 h Kalahari aging, representing a negligible impact in comparison to the significant effects observed in all other polymer types across various conditions. Representative images (after 2000 h Kalahari) of HIPS, LDPE, PA-6 and TPU are shown in Fig. 3. Both HIPS and PA-6 had rough surfaces with nano-sized divots or cracks after aging, while the LDPE particles showed µm-sized cracks in aged particles. The SEM images of the TPU indicated fragment release via surface ablation. The aged LDPE particles in Fig. 3 and SI Figs. 4 and 5 show distinct cracks over the full particle dimension indicating substantial degradation and the potential for fragmentation. The cracks in LDPE are shown to be approximately 10 µm in width, which is consistent across all 2000 h aged LDPE samples imaged. Similar observations on the formation of such micrometer-sized cracks in rooftop-aged LDPE samples (with and without rainwater) were noted by Miranda et al. [68]

Additionally, UV aging of HIPS, LDPE, and PA-6 by the three different aging protocols led to a reduction of the particle sizes compared to the pristine powders, while for TPU an increase of the particle sizes was detected (SI Fig. 6). As described above, TPU does not have a distinct melting peak, but a broad melting area and additionally crosslinking was observed. Our results imply that the pristine TPU particles might have softened and crosslinked during the treatment, leading to chemically bonded TPU agglomerates [70, 71].

Release kinetics for secondary micro- and nanoplastics and dissolved organics

Since the impact of the different UV aging protocols on the various types of microplastics investigated influenced the release rates of the degradation species (Fig. 1, secondary micro- and nanoplastics, dissolved organic carbon, DOC), a screening method was needed to decide which samples should be analyzed by the advanced techniques. In this study, we used the single particle counter to assess the release of secondary microplastics after all aging stresses were applied (SI Tables 7, 8, 9, 10 and 11). The heat map in Fig. 4 shows the impact of the aging protocols on the fragmentation of the microplastic types investigated, comparing the total counts detected.

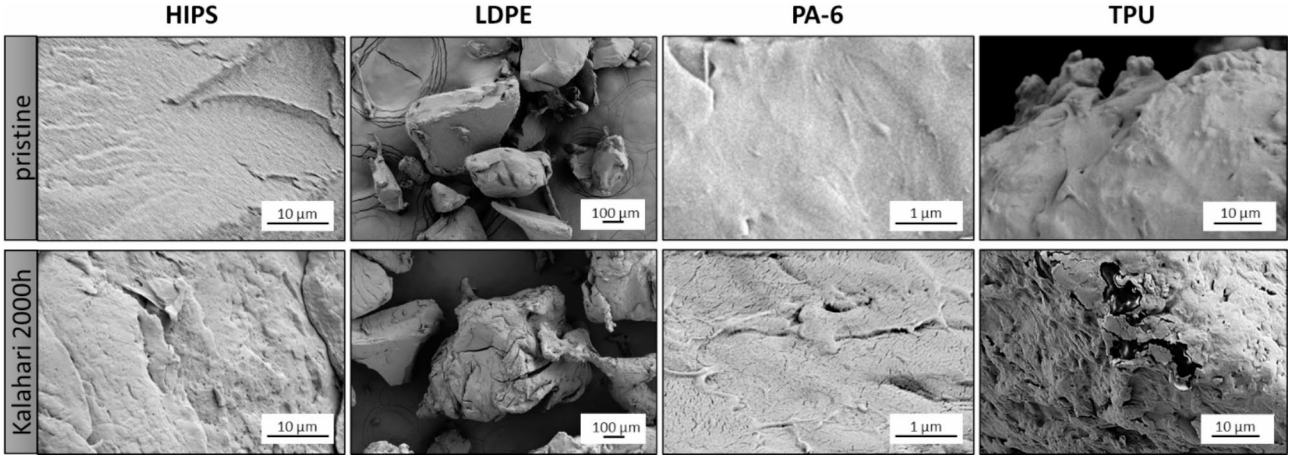

Fig. 3 Changes in the surface texture observed for HIPS, LDPE, PA-6 and TPU after 2000 h aging via Kalahari protocol

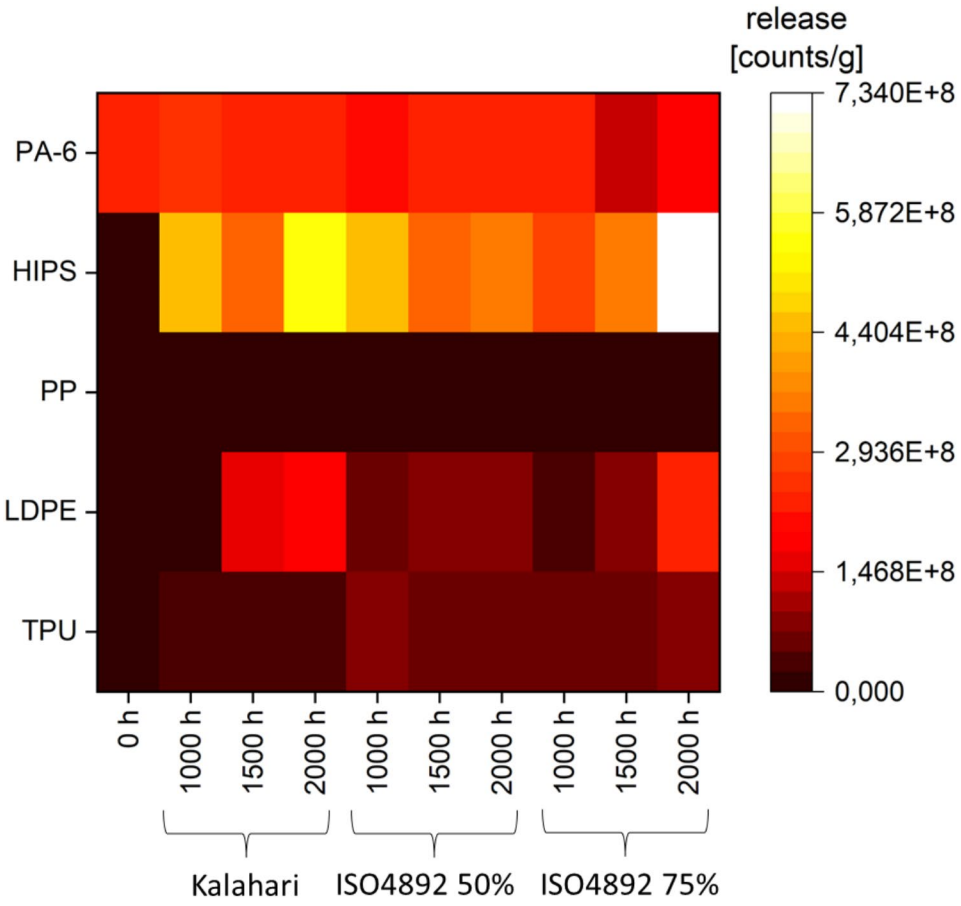

Fig. 4 Total particle counts per gram of plastic. Counts are summed up across the range from 1 to 139 µm, and the graph compares counts before and after UV aging from 5 different microplastic types by 3 different UV aging protocols and 3 timepoints. The UV aging protocols (Kalahari, ISO4892 50% and 75%) varied in temperature and relative humidity

For HIPS, LDPE, and TPU the total particle counts from the 1 to 139 µm range increased after UV aging, clearly showing the fragmentation of these materials and secondary microplastic release. HIPS showed the highest release of $7.3 \pm 3.1 \cdot 10^8$ counts per gram polymer after 2000 h aging via ISO4892, RH 75%, but this also had the broadest scatter in the duplicate measurements. The effect of the high temperature in the Kalahari protocol to HIPS also led to a high release of $5.4 \pm 0.2 \cdot 10^8$ counts per gram polymer and even the lowest recorded release of $2.8 \pm 0.4 \cdot 10^8$ counts per gram polymer (after 1000 h aging with ISO4892, RH 75% protocol) was still higher than any release from the other microplastic types in any protocol tested. In the case of LDPE, fragmentation was more pronounced at higher UV aging temperature (Kalahari 2000 h: $1.8 \pm 0.3 \cdot 10^8$ counts per gram polymer) and with increasing duration of the UV treatment. This trend was not observed for HIPS treated by Kalahari and ISO4892, RH 50%. Here, the fragmentation was higher after 1000 h, then lower after 1500 h and higher again after 2000 h UV treatment. This might be supported by the published surface ablation mechanism introduced by A. Andrady [35]: After 1000 h UV treatment, the HIPS surface fragments and secondary microplastics are released. Before the next surface layer can be affected, the previously formed fragments need to be removed from the particle surface or further degraded into nanoplastics and other species. This assumption is supported by measurements of the carbonyl index before and after NanoRelease (HIPS, 2000 h ISO4892, RH 50%) showing a reduction of the carbonyl index value by 3.5% after removal of the outermost aged layer. This observation was even more pronounced for LDPE (2000 h ISO4892, RH 50%), where the carbonyl index was reduced by 23.8% after the NanoRelease treatment. Specifically for HIPS, the blend structure can also influence its fragmentation. While the matrix consists of polystyrene, the dispersed phase is based on butadiene rubber. The two polymer types are affected differently by UV aging stresses, which highlights the high potential for defect formation or release of the dispersed phase as secondary micro- or nanoplastics, as observed with Carbon Black or silica fillers [72–74]. The aromatic TPU showed low, albeit consistent and measurable, secondary fragment release that increased as UV duration increased.

In this case, the release was higher in presence of water (both ISO4892 protocols). In the absence of water, the molecular weight reduction was more pronounced for the investigated TPU, while the carbonyl index was higher in the presence of water. This might indicate that higher temperatures and low humidity lead to the formation of low-molecular polymer chains that would not be released as solid particles [75], while conversely in this polymer the presence of water molecules favors fragmentation. For PP and PA-6 no increase or decrease in the total particle counts between 1 and 139 µm were detected after all UV aging stresses applied. Since the molecular mass reduction was low for PP and no increase of the carbonyl index detected (Fig. 2a + b), we assume that the aging duration (and thus accumulated UV dose) was not sufficient to overcome the UV stabilizing additives and induce severe aging of this material. In case of the PA-6, however, the molar mass was drastically reduced and changes in the carbonyl index were detected (Fig. 2a + b). Furthermore, the size distribution of PA-6 was changed after treatment with both ISO4892 protocols (Fig. 5a). Specifically, after UV aging under ISO4892, RH = 50% conditions, we observed a notable increase in the number of particles measuring approximately 1 µm. This increase surpassed the total count of 1 µm particles found in the pristine powder, while simultaneously, the total counts of larger particles were significantly reduced. Treatment with ISO4892, RH 75% led exclusively to a reduction in the total particle counts of fragments sized between 4 and 30 µm. In contrast, for HIPS, the total particle counts across all size categories increased following any UV treatment (Fig. 5b). Assuming spherical particles, we converted the total particle counts into a mass (separately for each size fraction). This allowed us to compare the various protocols and timepoints against the initial mass of fragments sized between 1 and 139 µm, as depicted in Fig. 5c. From this analysis, the difference in the fragmentation and degradation mechanisms of PA-6 and HIPS becomes evident. Notably, PA-6 absorbs water during UV aging [63], facilitating bulk degradation. We interpret that this process results in shrinkage due to bulk volume loss with predominant release of DOC (Fig. 1), ultimately

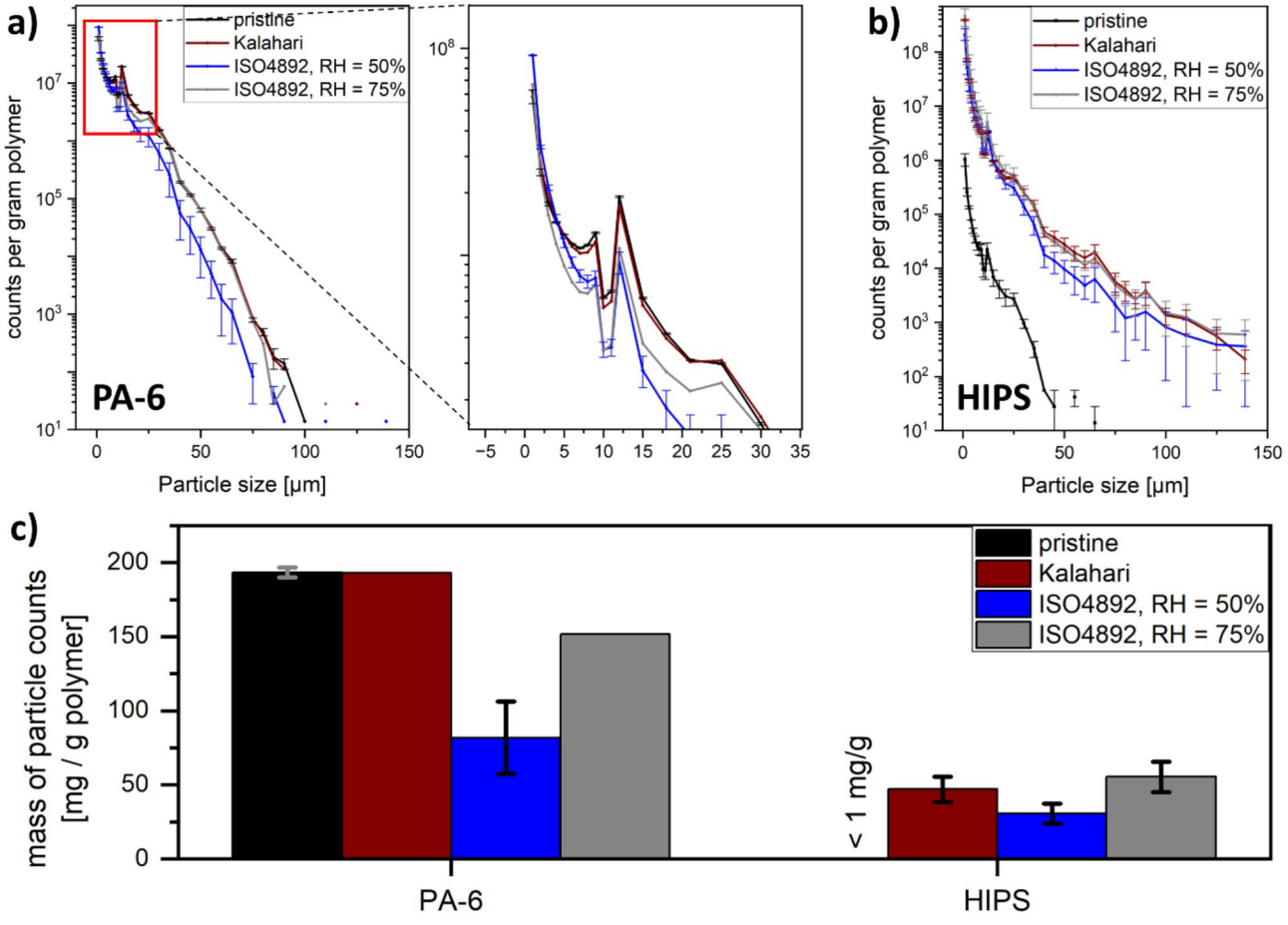

Fig. 5 Total particle counts 1–139 µm detected for (**a**) PA-6 and (**b**) HIPS before and after 2000 h UV aging by three different UV aging protocols (Kalahari, ISO4892 RH = 50% and RH = 75%). (**c**) Conversion of the total particle counts (each size bin separately) into a total mass. PA-6 and HIPS were selected among all types of polymers investigated to emphasize the differences in potential fragmentation patterns

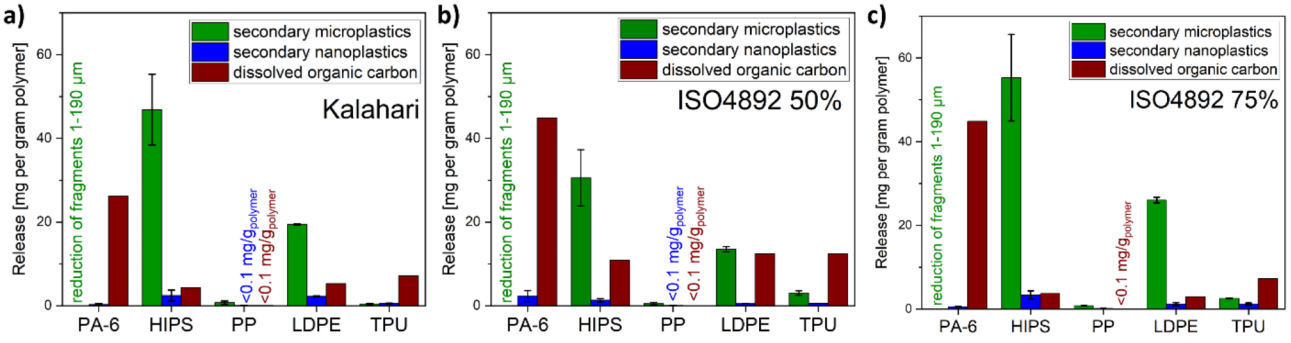

Fig. 6 Comparison of releases in mg per gram polymer of different release species (secondary microplastics, secondary nanoplastics, dissolved organic carbon) after 2000 h aging with different UV aging protocols, values of pristine material subtracted; (**a**) Kalahari, (**b**) ISO4892, RH = 50%, (**c**) ISO4892, RH = 75%. For PA-6 the "microplastic release" was set to zero because only overall particle shrinkage (i.e., less mass) was detected after UV aging compared to the pristine material (compare to Fig. 5)

leading to a reduction in both particle sizes and total particle counts. In contrast, we rationalize the findings on HIPS by fragmentation as the dominating mechanism during UV treatment, attributed to surface ablation and release of daughter fragments (Fig. 1), thus explaining that total particle counts, and mass of fragments increased compared to the pristine material. Notably, the total particle counts of released fragments from HIPS are higher than from PA-6, but the total mass is lower due to the smaller sizes of fragments released. Previous findings on PA-6 are explicable by the same mechanism [36], and are consistent with the observed increase in 1 µm counts and nanoplastic release from PA-6 after 2000 h UV aging without humidity control, followed by the disappearance of these fragments after 3000 h (Reference 36, Fig. 4).

Several authors concluded that the UV aging of microplastics not only leads to the release of solid secondary micro- and nanoplastics, but also leads to the release of DOC (Fig. 1) [36, 37, 76–79]. It is important to note that DOC is only detectable in the closed laboratory environment, not in environmental monitoring studies, due to filter sampling. The new data reported in this study shows how each polymer has distinct patterns of degradation into secondary microplastics, secondary nanoplastics, and DOC (Fig. 6, SI Table 12), and that pattern was additionally modulated by humidity and temperature (Fig. 6a, b,c and SI Table 12), but remained overall remarkably characteristic of each respective polymer. For PP, low releases of all species after all UV aging conditions were detected, which also fits to the low changes in chemical degradation observed for this material. As mentioned before, the dominating transformation mechanism of HIPS is fragmentation in all UV aging protocols, due to the high release of microplastic fragments and low release of DOC and is also the case for LDPE. For both materials the ISO4892 protocol with RH 50% led to higher DOC release and reduced secondary microplastic release compared to the other protocols. Increased fragmentation of LDPE in presence of rainwater was also observed by Miranda et al. [68] For PA-6 and TPU, the dominating transformation mechanism is dissolution, due to the high release of DOC and low release of micro- and nanoplastic fragments. In the case of TPU, we observed that the presence of water favors fragmentation, while the DOC release remains stable. With PA-6, we detected that larger microplastic fragments disappear with extended aging (Fig. 5a), in parallel to a low mass transfer to nanoplastics and high mass transfer to DOC: The observations suggest particle shrinkage with predominant dissolution and limited fragmentation. SI Fig. 6 in our previous publication [36] shows how nanoplastics were formed on the surface of the larger PA-6 particles (probably due to inhomogeneity in aging and non-uniformity of particles) after UV aging, but the half-life of formed nanoplastics remains unclear. In the case of PA-6 the presence of water during UV aging (ISO4892 vs. Kalahari) led to higher release of DOC. Overall, we conclude that the polymer type was the main factor affecting micro- and nanoplastic or DOC release, with minimal variations within the aging protocols. Statistical tests could further confirm the significance of polymer types or aging protocols on degradation outcomes [80].

Conclusion

In this study, several environmental stressors (UV, humidity, temperature) were applied with varying time periods to assess the release products from different types of polymers due to environmental aging. While the variation of the aging protocols slightly influenced the release of DOC, micro- and nanoplastics, the polymer composition dictated the species and amount of release products. Comparing both ISO4892 protocols, the presence of water contributed to radical termination mechanisms [62] which led for HIPS, LDPE and TPU to lower carbonyl indices and DOC release, but higher releases of micro- and nanoplastics. The aging and fragmentation

mechanism of PA-6 differed from those of the other polymers, probably due to its capability to take up water: [36] instead of fragmentation, we observed a particle shrinkage mechanism, which is accelerated with increasing humidity, leading to higher DOC release. The Kalahari protocol operates at higher temperature, which should accelerate the aging [62], but at lower humidity than the ISO4892 protocols. In consequence, for LDPE and HIPS the amount of released fragments was in between the release of both ISO4892 protocols. The DOC release from PA-6 was lower after Kalahari, since its main degradation mechanism is dictated by the presence of water. SI Fig. 7 shows the lack of a simple correlation between plastic degradation (here: carbonyl index) and fragmentation (here: microplastic counts), and instead highlights polymer-specific trends. The selection of polymer types was guided by the objective of including a wide range of materials that were expected to behave differently during aging and fragmentation. In this context, HIPS was chosen over PS due to the phase separation present in its original structure, which introduces a new aspect influencing the fragmentation of this material. Additionally, a stabilized PP was included as negative control. By comparing our results with existing literature [59, 81], we can affirm the significant impact of stabilizing additives in preventing or at least slowing down the fragmentation and degradation of PP. In general, insights such as those from this study and others support Safe and Sustainable by Design strategies for new product developments by selecting material-additive combinations with low micro- and nanoplastic release or even low release of any species due to high polymer stability enhanced by stabilizing additives.

In the context of environmental risk, it is important that the potential release of additives is also considered alongside release of the polymeric material [82]. This study did not consider additives, but it is worth noting that our negative control, PP, had low releases of all species due to the addition of UV stabilizing additives. While low polymer particle release has to be considered as just one category of the overall environmental lifecycle impact, we did not assess additives contained or released from the microplastic particles in this study, nor did we assess the impact of UV stabilizing additives on the other polymer compositions studied here. Work is currently ongoing to build predictive tools for additive release, which when combined with degradation and fragmentation modeling enabled by this study, will provide a powerful tool for assessing environmental risk.

Furthermore, it needs to be mentioned that this study was conducted in a controlled laboratory environment, and therefore cannot be directly compared to the complex conditions found in the environment. However, such comparisons of polymer types are only possible under well-defined conditions. Consequently, a comprehensive understanding of the fate of micro- and nanoplastics in the environment requires a combination of harmonized and standardized laboratory studies, field testing, and modeling. This complex issue cannot be addressed by a single study. Rather, a collaborative and ongoing effort among various researchers is needed. Currently, plastic fate and exposure models treat fragmentation simplistically (for example, using a constant fragmentation rate across degradation state and polymer size), or not at all [22, 83–86]. Even models that include fragmentation often do so as a loss process, which ignores size-differential risk posed by smaller plastic particles, and ignores the loss of particle character for dissolved organics. This study, among others, clearly demonstrates the importance of a more refined approach to fragmentation modeling that considers degradation stresses encountered by plastics in the environment. It emphasizes the importance of tracking the full size-distribution of secondary plastic particles and low-molecular-weight species, considering also different fragmentation patterns as e.g., particle shrinkage vs. bulk and surface fragmentation, as observed in this study. Depending on the fragmentation mechanism (surface ablation or bulk fragmentation), the preferred metric for expressing releases may differ, with normalization by mass or density being suitable for bulk fragmentation, and normalization by surface area for surface ablation. The data presented herein provide an excellent basis on which to build such a modeling approach for environments with intense UV stress, enabling the generation of fragmentation rates and fragment size distributions that are a function of polymer type, additives package, shape (particle, pellet, film, molded article…), the pristine polymer molar mass distribution, particle size and degradation state. A model for the mass transfer between different particle sizes and DOC (FRAGMENT-MNP) is currently parameterized based on the data discussed in this study [52]. Further research should focus on generating additional datasets with similar techniques by e.g. comparing polymers with different additive packages or different environmental conditions. By linking the degradation state to stresses encountered in the environment, modelers can scale fragmentation rates according to which environmental compartment plastics are present in, enabling predictive calculations of fragmentation in the environment. For example, in the context of UV aging, plastic particles present in the atmosphere or at the surface of waterbodies are likely to undergo UV aging, whilst particles buried deep in soils will see little UV light (where other stresses, such as biodegradation, are more important). Integrating these refined fragmentation predictions into exposure models is crucial in enabling the environmental risk assessment of polymers

that considers the full heterogeneity of plastics in the environment.

Abbreviations

ATR FT-IR	Attenuated total reflectance Fourier-transform infrared spectroscopy
AUC-RI	Analytical ultracentrifugation with refractive index detector
ΔH_m	Melt enthalpy
DOC	Dissolved organic carbon
DSC	Differential scanning calorimetry
GPC	Gel permeation chromatography
HIPS	High impact polystyrene
LDPE	Low density polyethylene
M_n	Number average molecular weight
M_w	Mass average molecular weight
PP	Polypropylene
PA	Polyamide
SDS	Sodium dodecyl sulfate
SEM	Scanning electron microscopy
T_g	Glass transition temperature
T_m	Melting point
TPU	Thermoplastic polyurethane
UV	Ultraviolet

Supplementary Information

The online version contains supplementary material available at https://doi.org/10.1186/s43591-025-00118-9.

Supplementary Material 1: Additional information on technical properties of the polymers, micrographs of pristine and aged polymers, descriptions of analytical methods and controls, characterization of the investigated polymers before and after UV aging (DSC, GPC, Fraunhofer diffraction), determined releases from AUC, particle counter and DOC, correlation-plot: Δcounts of microplastics vs. carbonyl index increase (PDF)

Acknowledgements

The authors sincerely thank Klaus Vilsmeier, Tanja Kiessig, Elke Schumacher, and Alexandre Tetrault for extensive data generation. We are also grateful to Maik Nowak (DSC), Rolf Tompers (DOC) and Bastiaan Staal (GPC on HIPS, TPU, PA) for their scientific advice on polymer analytics and to our project partners Antonia Prätorius (University of Amsterdam), Richard Cross and Gbotemi Adediran (UKCEH) for in depth discussions. We are especially thankful to Dow (David Meunier, Jing Hu, Jingwei Fan, Sarah Pei, Paul Balding, Jianbo Hou, Intan Hamdan) and LyondellBasell (Erik Rushton, Isabella Camurati, Mara Destro, Gabriele Tani) for their outstanding effort in the GPC analysis of partially UV degraded, fragmented, and crosslinked polyolefins.

Author contributions

The manuscript was written and revised through contributions of all authors. All authors have given approval to the final version of the manuscript. PP and KS contributed equally to this work. KS and JS carried out the experiments for this study. SH and MW performed the data curation for modelling purposes. PP wrote the original draft with contributions from KS, JS, MW, SH, CS and WW. All authors approved the final version of the manuscript. WW, CS and MW supervised the project.

Funding

This work was supported by Cefic Long Range Research Initiative under project LRI ECO59 (FRAGMENT-MNP).

Data availability

The authors declare that the data supporting the findings of this study are available within the paper and its Supplementary Information files. Should any raw data files be needed in another format they are available from the corresponding author upon reasonable request.

Declarations

Ethics approval and consent to participate

Not applicable.

Consent for publication

All authors have given approval to the final version of the manuscript.

Competing interests

Some of the authors are employees of BASF SE, a company producing and marketing polymers, including plastics.

Received: 11 October 2024 / Accepted: 23 February 2025
Published online: 06 March 2025

References

1. Thompson RC, Olsen Y, Mitchell RP, Davis A, Rowland SJ, John AWG, McGonigle D, Russell AE. Lost at sea: where is all the plastic?? Science. 2004;304:838.
2. Kedzierski M, Cirederf-Boulant D, Palazot M, Yvin M, Bruzaud S. Continents of plastics: an estimate of the stock of microplastics in agricultural soils. Sci Total Environ. 2023;880:163294. https://doi.org/10.1016/j.scitotenv.2023.163294
3. Batool I, Qadir A, Levermore JM, Kelly FJ. Dynamics of airborne microplastics, appraisal and distributional behaviour in atmosphere; a review. Sci Total Environ. 2022;806:150745. https://doi.org/10.1016/j.scitotenv.2021.150745
4. Bergmann M, Mützel S, Primpke S, Tekman MB, Trachsel J, Gerdts G. White and wonderful? Microplastics prevail in snow from the alps to the Arctic. Sci Adv. 2019;5:eaax1157.
5. Rummel CD, Jahnke A, Gorokhova E, Kühnel D, Schmitt-Jansen M. Impacts of biofilm formation on the fate and potential effects of microplastic in the aquatic environment. Environ Sci Technol Lett. 2017;4:258–67. https://doi.org/10.1021/acs.estlett.7b00164
6. Rocha-Santos T, Duarte AC. A critical overview of the analytical approaches to the occurrence, the fate and the behavior of microplastics in the environment. TRAC Trends Anal Chem. 2015;65:47–53. https://doi.org/10.1016/j.trac.2014.10.011
7. Ward CP, Reddy CM, Opinion. We need better data about the environmental persistence of plastic goods. Proc Natl Acad Sci U S A. 2020;117:14618–21. https://doi.org/10.1073/pnas.2008009117
8. Chamas A, Moon H, Zheng J, Qiu Y, Tabassum T, Jang JH, Abu-Omar M, Scott SL, Suh S. Degradation rates of plastics in the environment. ACS Sustain Chem Eng. 2020;8:3494–511. https://doi.org/10.1021/acssuschemeng.9b06635
9. Andrady AL. in *Marine Anthropogenic Litter* (eds M. Bergmann, L. Gutow, & M-Klages) 57–72 2015.
10. Lehner R, Weder C, Petri-Fink A, Rothen-Rutishauser B. Emergence of nanoplastic in the environment and possible impact on human health. Environ Sci Technol. 2019;53:1748–65. https://doi.org/10.1021/acs.est.8b05512
11. Wang L, Wu W-M, Bolan NS, Tsang DCW, Li Y, Qin M, Hou D. Environmental fate, toxicity and risk management strategies of nanoplastics in the environment: current status and future perspectives. J Hazard Mater. 2021;401:123415. https://doi.org/10.1016/j.jhazmat.2020.123415
12. Huber MJ, Ivleva NP, Booth AM, Beer I, Bianchi I, Drexel R, Geiss O, Mehn D, Meier F, Molska A, Parot J, Sorensen L, Vella G, Prina-Mello A, Vogel R, Caputo F. Physicochemical characterization and quantification of nanoplastics: applicability, limitations and complementarity of batch and fractionation methods. Anal Bioanal Chem. 2023;415:3007–31. https://doi.org/10.1007/s00216-023-04689-5
13. Wohlleben W, Bossa N, Mitrano DM, Scott K. Everything falls apart: How solids degrade and release nanomaterials, composite fragments, and microplastics. NanoImpact. 2024;34:100510. https://doi.org/10.1016/j.impact.2024.100510
14. Yu Y, Flury M. How to take representative samples to quantify microplastic particles in soil? Sci Total Environ. 2021;784. https://doi.org/10.1016/j.scitotenv.2021.147166
15. Eich A, Mildenberger T, Laforsch C, Weber M. Biofilm and diatom succession on polyethylene (PE) and biodegradable plastic bags in two marine habitats: early signs of degradation in the pelagic and benthic zone?? PLoS ONE. 2015;10:e0137201. https://doi.org/10.1371/journal.pone.0137201
16. Prata JC, Reis V, da Costa JP, Mouneyrac C, Duarte AC, Rocha-Santos T. Contamination issues as a challenge in quality control and quality assurance in

microplastics analytics. J Hazard Mater. 2021;403:123660. https://doi.org/10.1016/j.jhazmat.2020.123660
17. Gwinnett C, Miller RZ. Are we contaminating our samples? A preliminary study to investigate procedural contamination during field sampling and processing for microplastic and anthropogenic microparticles. Mar Pollut Bull. 2021;173:113095. https://doi.org/10.1016/j.marpolbul.2021.113095
18. Amobonye A, Bhagwat P, Singh S, Pillai S. Plastic biodegradation: frontline microbes and their enzymes. Sci Total Environ. 2021;759:143536. https://doi.org/10.1016/j.scitotenv.2020.143536
19. Liu L, Xu M, Ye Y, Zhang B. On the degradation of (micro)plastics: degradation methods, influencing factors, environmental impacts. Sci Total Environ. 2022;806:151312. https://doi.org/10.1016/j.scitotenv.2021.151312
20. Pfohl P, Roth C, Meyer L, Heinemeyer U, Gruendling T, Lang C, Nestle N, Hofmann T, Wohlleben W, Jessl S. Microplastic extraction protocols can impact the polymer structure. Microplastics Nanoplastics. 2021;1. https://doi.org/10.1186/s43591-021-00009-9
21. Cashman MA, Ho KT, Boving TB, Russo S, Robinson S, Burgess RM. Comparison of microplastic isolation and extraction procedures from marine sediments. Mar Pollut Bull. 2020;159:111507. https://doi.org/10.1016/j.marpolbul.2020.111507
22. Domercq P, Praetorius A, MacLeod M. The full multi: an open-source framework for modelling the transport and fate of nano- and microplastics in aquatic systems. Environ Model Softw. 2022;148:105291. https://doi.org/10.1016/j.envsoft.2021.105291
23. Harrison S, Cross R, Wohlleben W, Pfohl P, Wiesner MR, Praetorius A, Santizo KY, Sipe JM, Adediran G, Svendsen C. FRAGMENT-MNP: Developing a mechanistic model of Micro and NanoPlastic FRAGMentation in the ENvironmenT. 22nd Annual Cefic-LRI Workshop, Brussels, Belgium, 8–9 November 2021, 2021. https://doi.org/10.5281/zenodo.5708123
24. Chaupart N, Serpe G, Verdu J. Molecular weight distribution and mass changes during polyamide hydrolysis. Polymer. 1998;39:1375–80.
25. Tamayo-Belda M, Pulido-Reyes G, Gonzalez-Pleiter M, Martin-Betancor K, Leganes F, Rosal R, Fernandez-Pinas F. Identification and toxicity towards aquatic primary producers of the smallest fractions released from hydrolytic degradation of polycaprolactone microplastics. Chemosphere. 2022;303:134966. https://doi.org/10.1016/j.chemosphere.2022.134966
26. Ainali NM, Bikiaris DN, Lambropoulou DA. Aging effects on low- and high-density polyethylene, polypropylene and polystyrene under UV irradiation: an insight into decomposition mechanism by Py-GC/MS for microplastic analysis. J Anal Appl Pyrol. 2021;158. https://doi.org/10.1016/j.jaap.2021.105207
27. Scholz P, Wachtendorf V, Panne U, Weidner SM. Degradation of MDI-based polyether and polyester-polyurethanes in various environments - effects on molecular mass and crosslinking. Polym Test. 2019;77:105881. https://doi.org/10.1016/j.polymertesting.2019.04.028
28. Zumstein MT, Rechsteiner D, Roduner N, Perz V, Ribitsch D, Guebitz GM, Kohler HE, McNeill K, Sander M. Enzymatic hydrolysis of polyester thin films at the nanoscale: effects of polyester structure and enzyme active-site accessibility. Environ Sci Technol. 2017;51:7476–85. https://doi.org/10.1021/acs.est.7b01330
29. Kaushal J, Khatri M, Arya SK. Recent insight into enzymatic degradation of plastics prevalent in the environment: a mini - review. Clean Eng Technol. 2021;2. https://doi.org/10.1016/j.clet.2021.100083
30. Gijsman P, Meijers G, Vitarelli G. Comparison of the UV-degradation chemistry of polypropylene, polyethylene, polyamide 6 and polybutylene terephthalate. Polym Degrad Stab. 1999;65:433–41.
31. ter Halle A, Ladirat L, Martignac M, Mingotaud AF, Boyron O, Perez E. To what extent are microplastics from the open ocean weathered? Environ Pollut. 2017;227:167–74.
32. Song YK, Hong SH, Jang M, Han GM, Jung SW, Shim WJ. Combined effects of UV exposure duration and mechanical abrasion on microplastic fragmentation by polymer type. Environ Sci Technol. 2017;51:4368–76. https://doi.org/10.1021/acs.est.6b06155
33. Sipe JM, Bossa N, Berger W, von Windheim N, Gall K, Wiesner MR. From bottle to microplastics: can we estimate how our plastic products are breaking down? Sci Total Environ. 2022;814:152460. https://doi.org/10.1016/j.scitotenv.2021.152460
34. Nozaki S, Hirai T, Higaki Y, Yoshinaga K, Kojio K, Takahara A. Effect of chain architecture of polyol with secondary hydroxyl group on aggregation structure and mechanical properties of polyurethane elastomer. Polymer. 2017;116:423–8. https://doi.org/10.1016/j.polymer.2017.03.031
35. Andrady AL. The plastic in microplastics: a review. Mar Pollut Bull. 2017;119:12–22.
36. Pfohl P, Wagner M, Meyer L, Domercq P, Praetorius A, Hüffer T, Hofmann T, Wohlleben W. Environmental degradation of microplastics: how to measure fragmentation rates to secondary micro- and nanoplastic fragments and dissociation into dissolved organics. Environ Sci Technol. 2022;56:11323–34. https://doi.org/10.1021/acs.est.2c01228
37. Albergamo V, Wohlleben W, Plata DL. Photochemical weathering of polyurethane microplastics produced complex and dynamic mixtures of dissolved organic chemicals. Environ Sci Process Impacts. 2023. https://doi.org/10.1039/d2em00415a
38. Menzel T, Meides N, Mauel A, Mansfeld U, Kretschmer W, Kuhn M, Herzig EM, Altstadt V, Strohriegl P, Senker J, Ruckdaschel H. Degradation of low-density polyethylene to nanoplastic particles by accelerated weathering. Sci Total Environ. 2022;826:154035. https://doi.org/10.1016/j.scitotenv.2022.154035
39. Zhu L, Zhao S, Bittar TB, Stubbins A, Li D. Photochemical dissolution of buoyant microplastics to dissolved organic carbon: rates and microbial impacts. J Hazard Mater. 2020;383:121065. https://doi.org/10.1016/j.jhazmat.2019.121065
40. Gewert B, Plassmann MM, MacLeod M. Pathways for degradation of plastic polymers floating in the marine environment. Environ Sci Process Impacts. 2015;17:1513–21. https://doi.org/10.1039/c5em00207a
41. Allen NS, Parkinson A. Ultraviolet derivative absorption spectra of nylon 6,6 - Effect of photolysis versus photoinduced oxidation. Polym Degrad Stab. 1982;4:239–44.
42. Hoyle CE, Kim K-J, No YG, Nelson GL. Photolysis of segmented polyurethanes. The role of Hard-Segment content and hydrogen bonding. J Appl Polym Sci. 1987;34:763–74.
43. Meides N, Menzel T, Poetzschner B, Loder MGJ, Mansfeld U, Strohriegl P, Altstaedt V, Senker J. Reconstructing the environmental degradation of polystyrene by accelerated weathering. Environ Sci Technol. 2021;55:7930–8. https://doi.org/10.1021/acs.est.0c07718
44. Liu Z, Zhu Y, Lv S, Shi Y, Dong S, Yan D, Zhu X, Peng R, Keller AA, Huang Y. Quantifying the dynamics of polystyrene microplastics UV-aging process. Environ Sci Technol Lett. 2021;9:50–6. https://doi.org/10.1021/acs.estlett.1c00888
45. Shi X, Chen Z, Liu X, Wei W, Ni BJ. The photochemical behaviors of microplastics through the lens of reactive oxygen species: photolysis mechanisms and enhancing photo-transformation of pollutants. Sci Total Environ. 2022;846:157498. https://doi.org/10.1016/j.scitotenv.2022.157498
46. Mitrano DM, Diamond ML, Kim J-H, Tam KC, Yang M, Wang Z. Balancing new approaches and harmonized techniques in nano- and microplastics research. Environ Sci Technol Lett. 2023. https://doi.org/10.1021/acs.estlett.3c00359
47. Alimi OS, Claveau-Mallet D, Kurusu RS, Lapointe M, Bayen S, Tufenkji N. Weathering pathways and protocols for environmentally relevant microplastics and nanoplastics: what are we missing? J Hazard Mater. 2021;423:126955. https://doi.org/10.1016/j.jhazmat.2021.126955
48. Wohlleben W, Kingston C, Carter J, Sahle-Demessie E, Vázquez-Campos S, Acrey B, Chen C-Y, Walton E, Egenolf H, Müller P, Zepp R. NanoRelease: pilot interlaboratory comparison of a weathering protocol applied to resilient and labile polymers with and without embedded carbon nanotubes. Carbon. 2017;113:346–60.
49. ISO/TR 22293:2021. Evaluation of methods for assessing the release of nanomaterials from commercial, nanomaterial-containing polymer composites. 2021.
50. PlasticsEurope. *Plastics - the facts 2023: An analysis of European plastics production, demand and waste data*, https://www.plasticseurope.org/, 2023).
51. Pfohl P, Bahl D, Rückel M, Wagner M, Meyer L, Bolduan P, Battagliarin G, Hüffer T, Zumstein M, Hofmann T, Wohlleben W. Effect of polymer properties on the biodegradation of polyurethane microplastics. Environ Sci Technol. 2022;56:16873–84. https://doi.org/10.1021/acs.est.2c05602
52. Harrison S, Lopez B, Wiesner M. *FRAGMENT-MNP [Computer software]* 2024. https://github.com/microplastics-cluster/fragment-mnp.
53. Normenausschuss Kunststoffe (Plastics Standards Committee), Technical Committee NA 054-01-04 AA Verhalten gegen Umwelteinflüsse. DIN EN ISO 4892-2: Plastics– Methods of exposure to laboratory light sources - Amendment A1:2009). European Committee for Standardization. 2009.
54. Ruggiero E, Vilsmeier K, Mueller P, Pulbere S, Wohlleben W. Environmental release from automotive coatings are similar for different (nano)forms of pigments. Environ Science: Nano. 2019;6:3039–48. https://doi.org/10.1039/c9en00227h

55. Lv Y, Huang Y, Yang J, Kong M, Yang H, Zhao J, Li G. Outdoor and accelerated laboratory weathering of polypropylene: a comparison and correlation study. Polym Degrad Stab. 2015;112:145–59.
56. Shemesh D, Lan Z, Gerber RB. Dynamics of triplet-state photochemistry of pentanal: mechanisms of Norrish I, Norrish II, and H abstraction reactions. J Phys Chem A. 2013;117:11711–24.
57. Feldmann D. Polymer weathering: photo-oxidation. J Polym Environ. 2002;10:163–73.
58. Garvey CJ, Imperor-Clerc M, Rouziere S, Gouadec G, Boyron O, Rowenczyk L, Mingotaud AF, Ter Halle A. Molecular-scale understanding of the embrittlement in polyethylene ocean debris. Environ Sci Technol. 2020;54:11173–81. https://doi.org/10.1021/acs.est.0c02095
59. Burrows S, Colwell J, Costanzo S, Kaserzon S, Okoffo E, Ribeiro F, O'Brien S, Toapanta T, Rauert C, Thomas KV, Galloway T. UV sources and plastic composition influence microplastic surface degradation: implications for plastic weathering studies. J Hazard Mater Adv. 2024;14. https://doi.org/10.1016/j.hazadv.2024.100428
60. Almond J, Sugumaar P, N Wenzel M, Hill G, Wallis C. Determination of the carbonyl index of polyethylene and polypropylene using specified area under band methodology with ATR-FTIR spectroscopy. e-Polymers. 2020;20:369–81. https://doi.org/10.1515/epoly-2020-0041
61. Rosu D, Rosu L, Cascaval CN. IR-change and yellowing of polyurethane as a result of UV irradiation. Polym Degrad Stab. 2009;94:591–6. https://doi.org/10.1016/j.polymdegradstab.2009.01.013
62. Rabek JF. Polymer photodegradation: mechanisms and experimental methods. Volume 1. Springer Science + Business Media Dordrecht; 1995.
63. Monson L, Braunwarth M, Extrand CW. Moisture absorption by various polyamides and their associated dimensional changes. J Appl Polym Sci. 2007;107:355–63. https://doi.org/10.1002/app.27057
64. Girois S, Audouin L, Verdu J, Delprat B, Marot G. Molecular weight changes during the photooxidation of isotactic polypropylene. Polym Degrad Stab. 1996;51:125–32.
65. Hiemenz PC, Lodge TP. *Polymer Chemistry*. Vol. Second Edition (CRC Press, Taylor & Francis Group, 2007).
66. Koltzenburg S, Maskos M, Nuyken O. Polymere: synthese, eigenschaften und anwendungen. Berlin Heidelberg: Springer-; 2014.
67. Hamid SH, Amin MB, Maadhah AG. Handbook of polymer degradation. Volume 1. New York: Marcel Dekker Inc; 1992.
68. Miranda MN, Sampaio MJ, Tavares PB, Silva AMT, Pereira MFR. Aging assessment of microplastics (LDPE, PET and uPVC) under urban environment stressors. Sci Total Environ. 2021;796:148914. https://doi.org/10.1016/j.scitotenv.2021.148914
69. Rodriguez AK, Mansoor B, Ayoub G, Colin X, Benzerga AA. Effect of UV-aging on the mechanical and fracture behavior of low density polyethylene. Polym Degrad Stab. 2020;180. https://doi.org/10.1016/j.polymdegradstab.2020.109185
70. Dadbakhsh S, Verbelen L, Vandeputte T, Strobbe D, Van Puyvelde P, Kruth J-P. Effect of powder size and shape on the SLS processability and mechanical properties of a TPU elastomer. Physics Procedia. 2016;83:971–80. https://doi.org/10.1016/j.phpro.2016.08.102
71. Sun J, Zheng H, Xiang H, Fan J, Jiang H. The surface degradation and release of microplastics from plastic films studied by UV radiation and mechanical abrasion. Sci Total Environ. 2022;838:156369. https://doi.org/10.1016/j.scitotenv.2022.156369
72. Nguyen T, Pellegrin B, Bernard C, Rabb S, Stuztman P, Gorham JM, Gu X, Yu LL, Chin JW. Characterization of surface accumulation and release of nanosilica during irradiation of polymer nanocomposites by ultraviolet light. J Nanosci Nanotechnol. 2012;12:6202–15. https://doi.org/10.1166/jnn.2012.6442
73. Wei XF, Nilsson F, Yin H, Hedenqvist MS. Microplastics originating from polymer blends: an emerging threat?? Environ Sci Technol. 2021;55:4190–3. https://doi.org/10.1021/acs.est.1c00588
74. Nguyen T, Wohlleben W, Sung L. in *Safety of Nanomaterials along their Lifecycle: Release, Exposure and Human Hazards*,Boca Raton, FL. 2014.
75. van Pelt WW, Goossens JG. Depolymerization behavior of thermoplastic poly(urethane) (TPU) and its dependence on initial molecular weight. Anal Chim Acta. 2007;604:69–75. https://doi.org/10.1016/j.aca.2007.05.035
76. Walsh AN, Reddy CM, Niles SF, McKenna AM, Hansel CM, Ward CP. Plastic formulation is an emerging control of its photochemical fate in the ocean. Environ Sci Technol. 2021;55:12383–92. https://doi.org/10.1021/acs.est.1c02272
77. Ward CP, Armstrong CJ, Walsh AN, Jackson JH, Reddy CM. Sunlight converts polystyrene to carbon dioxide and dissolved organic carbon. Environ Sci Technol Lett. 2019;6:669–74. https://doi.org/10.1021/acs.estlett.9b00532
78. Andrady AL, Law L, Donohue K, J., Koongolla B. Accelerated degradation of low-density polyethylene in air and in sea water. Sci Total Environ. 2022;811:151368. https://doi.org/10.1016/j.scitotenv.2021.151368
79. Tuttle E, Wiman C, Munoz S, Law KL, Stubbins A. Sunlight-driven photochemical removal of polypropylene microplastics from surface waters follows linear kinetics and does not result in fragmentation. Environ Sci Technol. 2024;58:5461–71. https://doi.org/10.1021/acs.est.3c07161
80. Binda G, Costa M, Supraha L, Spanu D, Vogelsang C, Leu E, Nizzetto L. Untangling the role of biotic and abiotic ageing of various environmental plastics toward the sorption of metals. Sci Total Environ. 2023;893:164807. https://doi.org/10.1016/j.scitotenv.2023.164807
81. Reineccius J, Schonke M, Waniek JJ. Abiotic long-term simulation of microplastic weathering pathways under different aqueous conditions. Environ Sci Technol. 2023;57:963–75. https://doi.org/10.1021/acs.est.2c05746
82. Wang Z, Praetorius A. Integrating a chemicals perspective into the global plastic treaty. Environ Sci Technol Lett. 2022;9:1000–6. https://doi.org/10.1021/acs.estlett.2c00763
83. MacLeod M, Domercq P, Harrison S, Praetorius A. Computational models to confront the complex pollution footprint of plastic in the environment. Nat Comput Sci. 2023;3:486–94. https://doi.org/10.1038/s43588-023-00445-y
84. Mennekes D, Nowack B. Predicting microplastic masses in river networks with high spatial resolution at country level. Nat Water. 2023;1:523–33. https://doi.org/10.1038/s44221-023-00090-9
85. Koelmans AA, Kooi M, Law KL, van Sebille E. All is not lost: deriving a top-down mass budget of plastic at sea. Environ Res Lett. 2017;12. https://doi.org/10.1088/1748-9326/aa9500
86. Quik JTK, Meesters JAJ, Koelmans AA. A multimedia model to estimate the environmental fate of microplastic particles. Sci Total Environ. 2023;882:163437. https://doi.org/10.1016/j.scitotenv.2023.163437

Publisher's note